Nucleation and Ordering of an Electrodeposited Two-Dimensional Crystal: Real-Time X-Ray Scattering and Electronic Measurements

A. C. Finnefrock, K. L. Ringland, and J. D. Brock
School of Applied & Engineering Physics and Materials Science Center, Cornell University, Ithaca, New York 14853

L. J. Buller and H. D. Abruña
Department of Chemistry and Materials Science Center, Cornell University, Ithaca, New York 14853
(Received 17 December 1997; revised manuscript received 2 June 1998)

We have studied *in situ* the ordering of a two-dimensional Cu-Cl crystal electrodeposited on a Pt(111) surface. We simultaneously measured x-ray scattering and chronoamperometric transients during Cu desorption and subsequent ordering of the Cu-Cl crystal. In all cases, the current transient occurs on a shorter time scale than the development of crystalline order. The ordering time diverges with applied potential, consistent with the nucleation and growth of two-dimensional islands. We see a time-dependent narrowing of the x-ray peak, corresponding to the growing islands. [S0031-9007(98)07423-7]

PACS numbers: 68.10.Jy, 61.10.2–i, 64.60.Qb, 82.65.2–i

The electrodeposition of metals onto solid surfaces is a key aspect of important technological processes such as electroplating and corrosion inhibition. The initial stages of adsorption (deposition), along with the growth mechanism, dictate the structure and properties of the deposit. In many cases, metal overlayers can be deposited onto a dissimilar metal substrate at a potential that is less negative than that required for bulk deposition (the Nernst potential). This underpotential deposition (UPD) is an important experimental technique for investigating the early stages of deposition, and the diverse factors that influence it, for several reasons. First, in contrast to vacuum-surface experiments, the electrochemical interface provides direct control over the chemical potential of adsorbed species. This has been recently exploited by Ocko and co-workers [1] to study two-dimensional Ising lattice dynamics. Second, the charge double layer produces enormous (up to 10^7 V/cm) electric fields, capable of driving surface rearrangements [2]. Third, UPD is generally reversible. It is thus possible to perform repeated measurements of a deposition/desorption transition while systematically varying the control parameters.

The strongest interaction in a UPD process is between the metal to be deposited and the substrate [3,4]. Thus, UPD is usually restricted to the deposition of one monolayer prior to the onset of bulk deposition; in some systems, however, up to three atomic layers can be deposited. Although the metal-substrate interaction usually dominates, other interactions can also be important. For example, strongly adsorbing anions in the electrolyte are particularly important as both anion-metal and anion-substrate interactions significantly affect UPD processes. Furthermore, the adsorbed species rarely loses its charge completely during the early stages of deposition [5–10]. Rather, it becomes completely reduced only when the applied potential is close to the Nernst potential. This variable charge state alters the electrostatic interaction between the deposit and the anions. At more positive potentials, there is a strong attractive electrostatic interaction that disappears as the metal is discharged. This attractive interaction can produce a metal-anion bilayer on the electrode surface at intermediate potentials [10–14].

The UPD of copper onto the (111) surface of platinum in the presence of chloride anions is a well-known example of a system exhibiting such an intermediate bilayer and the phase diagram has been well characterized experimentally. The voltammetric profile of the Cu/Cl/Pt(111) system is shown in Fig. 1a. This profile, and all data in this report, were collected *in situ* in our x-ray scattering cell with a thin solution layer consisting of 0.1 M $HClO_4$ as a supporting electrolyte, 1 mM Cu^{2+}, and 10 mM Cl^-. The current response exhibits two sharp and well-defined voltammetric peaks centered at about +0.47 and +0.32 V (vs Ag/AgCl). At the highest potentials, no copper is

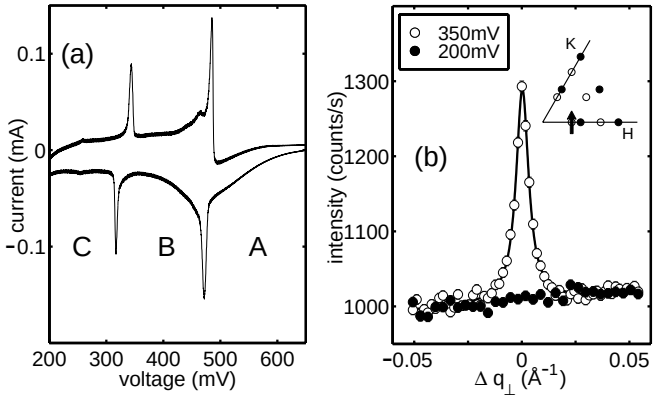

FIG. 1. (a) A cyclic voltammogram taken in the x-ray cell at a sweep rate of 5 mV/s. (b) Scattered intensity at $\boldsymbol{q} = (0.765\ 0\ 1.5) + \boldsymbol{q}_\perp$ at 350 and 200 mV (vs Ag/AgCl). The solid line is the best fit to a Lorentzian line shape.

believed to be present on the electrode surface, although chloride may be specifically adsorbed. As the voltage is decreased, the higher voltage peak corresponds to the initial formation of a Cu-Cl bilayer [14] which is *incommensurate* with the underlying Pt(111) lattice, and the lower voltage peak to the formation of a *commensurate* copper monolayer. The copper monolayer is, in turn, believed to be covered by a disordered layer of chloride anions [8,10,15–17]. Upon reversing the potential sweep direction, the current response then exhibits two sharp stripping peaks with only a small amount of hysteresis. In this Letter, we report simultaneous electrochemical and x-ray scattering measurements of the ordering kinetics of the Cu-Cl bilayer during the transition from the commensurate copper overlayer to the incommensurate bilayer. The data presented in this paper are consistent with a scenario in which the applied potential step desorbs the copper ions producing a transient in the current response and leaving a disordered overlayer of copper and chloride on the electrode surface. Subsequently, Cu-Cl grains nucleate and grow, producing the observed x-ray scattering signal.

The platinum crystal was prepared by repeated cycles of annealing and mechanical polishing [18]. Just prior to use, the Pt(111) surface was annealed in the flame of a propane torch and transferred to an *in situ* electrochemical x-ray cell, similar to those used by Toney and co-workers [19]. This design has only a thin layer of solution over the electrode to minimize the absorption of x rays and background scattering. The surface quality was checked by performing a cyclic voltammogram, as in Fig. 1a. The sharpness of these peaks is superior to many examples in the literature, and demonstrates that the quality of the electrochemical response is not compromised by the thin-layer geometry.

The Cu-Cl bilayer has an incommensurate hexagonal-close-packed structure [14]. Following Ref. [14], it is convenient to index reciprocal space using the lattice constant of bulk platinum and the standard notation [20] for the (111) surfaces of face-centered cubic crystals, where the (111) peak is mapped onto (003). For a nearly two-dimensional bilayer structure, the x-ray intensity will be sharp in H and K, and broad in L. An order parameter describing the transition is the intensity of the fundamental Cu-Cl Bragg rod at (0.765 0 L). Measurements of the remaining Bragg peaks are not necessary for studies of the kinetics of the ordering process. The Cu-Cl bilayer structure factor modulates the scattered intensity along the L axis and produces a maximum at $L \approx 1.5$. In our glancing angle geometry, the illuminated area of the electrode is largest for small values of L but the background scattering from and absorption by the solution layer are smallest at large values of L. Empirically, these considerations combine to produce a broad maximum in the signal-to-background ratio at $L \approx 1.5$. Because of the asymmetric spectrometer resolution, the rod is best resolved along a direction $\boldsymbol{q}_\perp$ orthogonal to (0.765 0) and at constant L. Figure 1b shows this overlayer Bragg peak intensity vs $\boldsymbol{q}_\perp$ at two different values of the applied potential. These data clearly demonstrate the presence of the incommensurate overlayer at 350 mV and its absence at 200 mV. The shape of the diffraction peak is well fit by a Lorentzian line shape, and the half width at half maximum Δ corresponds to a correlation length $\xi = 1/\Delta \sim 280$ Å. The potential-independent background is due to scattering from the solution layer and the polypropylene film which contains it. The inset indicates the location of the Bragg rods of the two-dimensional incommensurate overlayer (hollow) and the truncation rods [21] of the Pt substrate (filled). The arrow represents the transverse scan shown in the main figure.

An example of one of the square-wave potential cycles which we applied in order to study the stripping kinetics is shown in Fig. 2a. At $t = 0$, the potential begins at 200 mV. The voltage is stepped to 350 mV at $t =$ 10 sec. At $t = 30$ sec., the voltage is stepped back to 200 mV. This cycle repeats with a period of 40 sec. Throughout this cycle, we simultaneously monitor both the current (Fig. 2b) and the intensity of the scattered x rays (Fig. 2c) at a value of $\boldsymbol{q}_\perp$ which corresponds to the peak of Fig. 1b. To improve our signal-to-noise ratio, we integrate over several square-wave potential cycles. As expected, the incommensurate scattering peak is present only for values of the potential within the incommensurate phase. Note that the rise in the intensity of the scattered x-rays in Fig. 2c is much slower than the corresponding current transient in Fig. 2b. In contrast, the scattered intensity falls on a time scale similar to that of the current transient. The current transients describe the charge transfer at the electrode interface and have two components: the capacitive charging of the double layer, and the Faradaic charge transfer from the desorption/adsorption of ions. Since the rise in x-ray intensity is associated with the desorption of copper and the fall in x-ray intensity is associated with the deposition of copper, diffusion of copper between the surface and the bulk solution does not appear to be the rate-limiting step for the ordering kinetics. Moreover, the desorption process can be separated from the ordering process because of the widely disparate time scales involved.

Previous chronoamperometric studies of closely related systems [22] exhibit distinct features in the current response which have been interpreted as evidence of direct nucleation. These characteristic features are not present in our data. Therefore, our data suggest the scenario in which the Faradaic current response is due to simple desorption. The ordered phase nucleates and grows out of the remaining disordered overlayer. The difference between our measurements and previous measurements may be a result of cell geometry and is the subject of ongoing investigations.

In order to understand the kinetics of the ordering process, we need to access the full $\boldsymbol{q}$-t dependence of the x-ray scattering. To do this, we repeat the time-resolved measurement of Fig. 2 for a series of $\boldsymbol{q}$ points linearly spaced along $\boldsymbol{q}_\perp$, as indicated in the inset to Fig. 1b. An

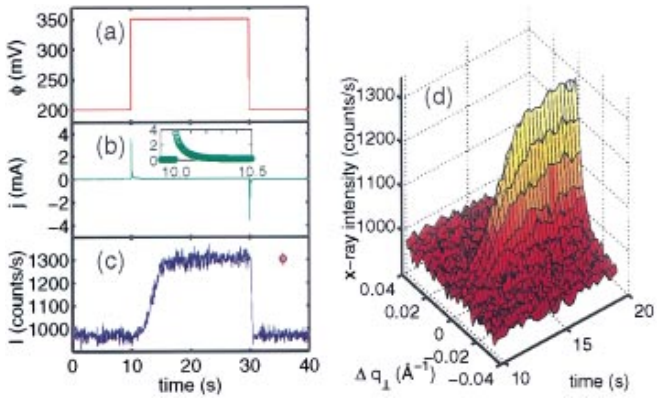

FIG. 2(color). (a) Applied potential steps. (b) Current transients. (c) Time dependence of the integrated intensity of the (0.765 0 1.5) overlayer diffraction peak. (d) Scattered intensity as a function of time t and transverse scattering vector $\boldsymbol{q}_\perp$ with a false color scale indicating intensity.

example of such a measurement is shown in Fig. 2d. The first thing to note is that the peak remains centered at a constant value of $\boldsymbol{q}_\perp$, ruling out the possibility that the overlayer simply shifts its periodicity in response to the change in potential. The correlation length is obtained from the width of the diffraction peak and is believed to be determined by the finite size of growing islands of Cu-Cl. The diffraction peak narrows with time, indicating that these islands are growing. The total surface coverage by the islands is proportional to the integrated intensity.

To begin our analysis of these data, we fit each time slice to a Lorentzian line shape. A Lorentzian is the lowest order approximation to the structure factor for any system with only short range positional order. The circles in Fig. 3a plot Δ and integrated intensity vs time. As expected for growing islands, Δ decreases and the integrated intensity increases monotonically with time.

We continue our analysis by considering a simple nucleation and growth model in which Cu-Cl islands

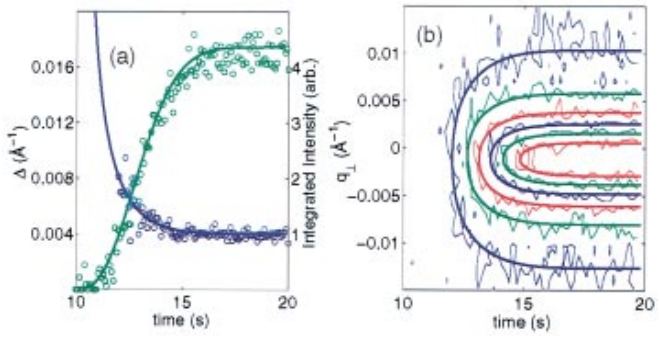

FIG. 3(color). (a) Best fit results for the half width at half maximum (Δ; blue) and the integrated intensity (I_0; green) vs time. Symbols are for a Lorentzian fit to a given time slice and the solid lines are for a Lorentzian constrained to have the Avrami form for the Δ and I_0. (b) Contours of constant intensity of the data set (thin lines) in Fig. 2d and from the best fit to the Avrami form (thick lines).

stochastically nucleate and then grow independently. The number of growing islands is assumed to be $N(t) = N_\infty(1 - e^{-k_N t})$ where N_∞ is the final number and k_N is a nucleation rate constant. Following the treatment of [23], if the area of an island nucleated at time t_0 is $A(t - t_0)$, the total "extended" area covered by all islands (ignoring overlap) is

$$\theta_{\text{ext}}(t) = N_\infty k_N \int_0^t dt_0\, A(t - t_0) e^{-k_N t_0}. \qquad (1)$$

As demonstrated by Avrami [24], the actual coverage θ is obtained from Eq. (1) using the relation $\theta = 1 - \exp(-\theta_{\text{ext}})$. Since a typical area scales as θ/N, a typical length scales as $\sqrt{\theta/N}$. Using these ideas, we refit the data set (Fig. 2d) to a single Lorentzian where we constrained the integrated intensity to be proportional to θ and the correlation length to be proportional to $\sqrt{\theta/N}$. The best fit of the entire data set (2×10^4 points) to this simple model produces a goodness-of-fit parameter $\chi^2 = 1.04$ and is summarized in Fig. 3b. The resulting integrated intensity and Δ functions are plotted as solid lines in Fig. 3a and agree well with our previous results where each time slice was fit independently. In sum, these kinetic x-ray data are quantitatively consistent with the nucleation and growth of a two-dimensional Cu-Cl bilayer.

We can extend our analysis further using elementary reaction rate theory, which predicts that $k_N = k_0 e^{-\Delta G_c/k_B T}$. Here, ΔG_c is the difference in the Gibbs free energy of a "critical" island and the same number of atoms in the disordered phase. Assuming direct desorption from an island into the solution,

$$\Delta G_c \sim \gamma^d (ze\eta)^{1-d}, \qquad (2)$$

where d is the spatial dimensionality of the island, γ is the surface energy of the island, ze is the charge on a metal ion, and η is the applied potential relative to its value at the transition. Equation (2) is the d-dimensional generalization of an expression derived in Ref. [23]. Alternatively, one obtains exactly the same expression if the desorption is described by a linearized Langmuir isotherm and the nucleation and growth is driven by the resulting change in coverage. Again, the absence of any features in our current response at the times associated with the nucleation of islands favors a two-step process but is not definitive due to the large capacitive-charging background.

In either scenario, we expect that as we quench deeper and deeper into the incommensurate phase, the transition will occur ever more rapidly. To test this hypothesis, we performed a series of voltage step measurements in which the applied potential was stepped from 200 mV (within the commensurate phase) to varying potentials within the incommensurate phase. As in the previous measurement, we measured the scattered intensity at the incommensurate overlayer peak position as a function of time. We characterized the transition time by fitting the x-ray intensity profiles (which resemble Fig. 2c) to a

trapezoidal functional form. While this model describes the data quite well, we ascribe no profound significance to it. Rather, we use it simply to define a characteristic time for the nucleation of islands, τ, which should be inversely proportional to k_N. The inset to Fig. 4 plots the best fit values of τ, which vary from 50 sec. for shallow quenches to 0.7 sec. for deep ones. Figure 4 illustrates the exponential dependence of τ on $1/\eta$, predicted by Eq. (2) with $d = 2$, over the entire phase region. The linear slope demonstrates that the growing islands are intrinsically two dimensional (rather than three-dimensional mounds or pits on the surface) and that these islands are compact rather than fractal. The range of τ is limited only by the phase diagram indicating that our thin solution layer has not inhibited the nucleation and growth processes. Furthermore, in all cases, τ is longer than the current transient time scale, which is insensitive to η.

In conclusion, we have studied a system wherein desorption (rather than deposition) is followed by ordering. The charge-transfer process is much faster than the development of long-range order. The x-ray data are well described by the nucleation and growth of two-dimensional islands. The potential-step experiments demonstrate that the rate of ordering agrees well with the nucleation and growth of two-dimensional islands over two decades in time, and is not limited by the thin-layer geometry. Further studies will explore the relationship between geometry-dependent diffusion processes, charge transfer at the interface, and nucleation mechanisms.

This work was supported by Cornell's Center for Materials Research (NSF Grant No. DMR-96-32275). Additional support was provided by the NSF (Grants No. DMR-92-57466 and No. CHE-94-07008) and the Office of Naval Research. The x-ray data were collected using the IBM-MIT beam line X20A at the National Synchrotron Light Source (NSLS), Brookhaven National Laboratory. NSLS is supported by the U.S. Department of Energy, Division of Materials Sciences and Division of Chemical Sciences. L. J. B. acknowledges financial support from the International Precious Metals Institute/Gemini Industries. A. C. F. thanks B. Ocko and M. Toney for numerous helpful discussions, and J. Jordan-Sweet at X20A.

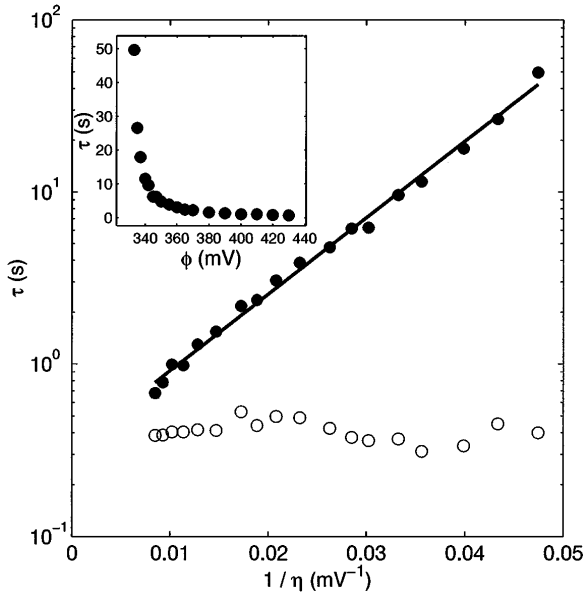

FIG. 4. Characteristic time vs applied voltage. Solid points represent x-ray transition times, while hollow points represent the time scale for the desorption current transient to fall to 5% of its peak value. The straight line is a fit to the nucleation model with $d = 2$. Inset: τ on a linear scale.

[1] B. M. Ocko, J. X. Wang, and T. Wandlowski, Phys. Rev. Lett. **79**, 1511 (1997).
[2] B. M. Ocko, J. Wang, A. Davenport, and H. Isaacs, Phys. Rev. Lett. **65**, 1466 (1990).
[3] D. Kolb, in *Advances in Electrochemistry and Electrochemical Engineering*, edited by H. Gerisher and C. Tobias (Wiley and Sons, New York, 1978), Vol. 11, p. 125; R. Adžić, *ibid.*, Vol. 13, p. 159.
[4] E. Budevski, G. Staikov, and W. Lorenz, *Electrochemical Phase Formation and Growth* (VCH Publishers, Weinheim, 1996).
[5] J. W. Schultze, Ber. Bunsenges. Phys. Chem. **74**, 705 (1970); J. W. Schultze and K. J. Vetter, J. Electroanal. Chem. **44**, 63 (1973).
[6] J. H. White and H. D. Abruña, J. Phys. Chem. **94**, 894 (1990).
[7] A. Tadjeddine, G. Tourillon, and D. Guay, Electochim. Acta **36**, 1859 (1991).
[8] N. Marković and P. N. Ross, Langmuir **9**, 580 (1993).
[9] S. Wu, J. Lipkowski, T. Tyliszczak, and A. P. Hitchcock, Prog. Surf. Sci. **50**, 227 (1995).
[10] H. S. Yee and H. D. Abruña, Langmuir **9**, 2460 (1993).
[11] Z. Shi, S. Wu, and J. Lipkowski, Electrochim. Acta **40**, 9 (1995).
[12] J. Li and H. D. Abruña, J. Phys. Chem. **101**, 244 (1997).
[13] M. F. Toney *et al.*, Phys. Rev. Lett. **75**, 4772 (1995).
[14] I. M. Tidswell, C. A. Lucas, N. M. Markovic, and P. N. Ross, Phys. Rev. B **51**, 10 205 (1995).
[15] D. M. Kolb, A. Jaff-Golze, and M. S. Zei, Dechema Monog. **102**, 53 (1986).
[16] H. Matsumoto, J. Inukai, and M. Ito, J. Electroanal. Chem. **379**, 223 (1994).
[17] R. Gómez *et al.*, Surf. Sci. **335**, 101 (1995).
[18] A. C. Finnefrock, Ph.D. dissertation, Cornell University, 1998.
[19] M. G. Samant *et al.*, Surf. Sci. Lett. **193**, L29 (1988).
[20] G. Grübel *et al.*, Phys. Rev. B **48**, 18 119 (1993).
[21] I. K. Robinson, Phys. Rev. B **33**, 3830 (1986).
[22] M. H. Hölzle, U. Retter, and D. M. Kolb, J. Electroanal. Chem. **371**, 101 (1994); M. H. Hölzle, V. Zwing, and D. M. Kolb, Electrochim. Acta **40**, 1237 (1995).
[23] W. Schmickler, *Interfacial Electrochemistry* (Oxford University Press, New York, 1996).
[24] M. Avrami, J. Chem. Phys. **7**, 1103 (1939); **8**, 212 (1940); **9**, 177 (1941).